

Research Article

A Wireless Sensor Network for Precise Volatile Organic Compound Monitoring

**Gianfranco Manes,¹ Giovanni Collodi,¹ Rosanna Fusco,²
Leonardo Gelpi,² and Antonio Manes³**

¹ *University of Florence and The MIDRA Consortium, 50139 Florence, Italy*

² *Health, Safety, Environment and Quality Department, Eni S.p.A., 00144 Rome, Italy*

³ *Netsens s.r.l, Sesto Fiorentino, 50019 Florence, Italy*

Correspondence should be addressed to Gianfranco Manes, gianfranco.manes@unifi.it

Received 24 November 2011; Accepted 8 February 2012

Academic Editor: Carlos Ramos

Copyright © 2012 Gianfranco Manes et al. This is an open access article distributed under the Creative Commons Attribution License, which permits unrestricted use, distribution, and reproduction in any medium, provided the original work is properly cited.

A variety of methods have been developed to monitor VOC concentration in hazardous sites. The methods range from calculation to measurement, point measuring to remote sensing. Some are suited for leak detection, others for estimation of the annual emission or both. None of the following available methods comes close to the ideal method. A distributed instrument providing precise monitoring of Volatile Organic Compound (VOC) concentration in a petrochemical plant is described; it consists of a Wireless Sensor Network (WSN) platform whose nodes are equipped with meteorological/climatic sensors and VOC detectors. Internet connectivity is provided in real time at a one-minute sampling rate, thus providing environmental authorities and plant management with an unprecedented tool for immediate warning in case of critical events. The paper describes the WSN platform, detailing various units (gateways, nodes, detectors) and shows the features of scalability and reconfigurability, with minimal intrusiveness or obtrusiveness. Environmental and process data are forwarded to a remote server and made available to the authenticated users through a rich user interface that provides data rendering in various formats and worldwide access to data. A survey of the VOC detector technologies involved is also provided.

1. Introduction

Volatile Organic Compounds (VOCs) are widely used in industries as solvents or chemical intermediates. Unfortunately, they include components which, if present in the atmosphere, may represent a risk factor for human health. VOCs are also found as contaminants or as byproducts of many processes, that is, in combustion gas stacks and groundwater clean-up systems. Benzene, for example, is highly toxic beyond a Time-Weighted Average (TWA) limit of 0.5 ppm (parts per million), as compared, for instance, with the TWA limit for gasoline, which is in the range of 300 ppm. Detection of VOCs at subppm levels is, thus, of paramount importance for human safety, and, consequently, critical for industrial hygiene in hazardous environments.

The most commonly used portable field instruments for VOC detection are the hand-held Photo-Ionisation Detectors (PIDs), which may be fitted with prefilter tubes

for specific gas detection. The pluses are that PIDs are accurate to subppm levels and measurements are fast, in the range of one or two minutes; for these reasons hand-held PIDs are well-suited to on-field operation. However, they have two drawbacks: they require skilled personnel and they cannot provide continuous monitoring. Wireless hand-held PIDs have recently become available on the market, thus overcoming these limitations, but they have a limited battery life, in addition to being relatively costly. This paper describes the implementation and on-field results of an end-to-end distributed monitoring system using VOC detectors which are capable of performing real-time analyses of gas concentrations in potentially hazardous sites on an unprecedented time/space scale [1].

Wireless sensor networks (WSNs), equipped with various gas sensors, have been actively used for air quality monitoring in the first decade of the 2000s [2–4]. WSNs have the advantage of offering full coverage of the terrain under



FIGURE 1: Installation overview. The grey circles indicate the position of each SNU; the blue arrows show wind direction.

inspection by collecting measurements from redundant portions of the zone. WSNs are thus the ideal instrument for specific and efficient environmental VOC monitoring [5, 6]. This paper describes the implementation of just such a system: a distributed network for precise VOC monitoring installed in a potentially hazardous environment. The system consists of a WSN infrastructure with nodes equipped with both weather/temperature sensors as well as VOC detectors and fitted with TCP/IP over GPRS Gateways to forward the sensors' data via Internet to a remote server. A user interface then provides access to the data as well as offering various formats of data rendering. This prototype was installed in the eni Polimeri Europa (PEM) chemical plant in Mantova, Italy, where it has been in continuous and unattended operation since April 2011. This pilot site is testing and assessing both the communications and the VOC detection technologies.

To avoid excavations, a stand-alone system, that is, one relying only on autonomous energy and connectivity resources, was designed and installed. In terms of energy requirements, the VOC detectors proved to be, by far, the greatest energy user, compared to the computational and communication units. So, to ensure a sustainable battery life for the deployed units, efficient power management strategies were studied and implemented; moreover, the WSN elements were equipped with a secondary energy source, consisting of a photovoltaic panel.

2. System Overview

A general overview of the deployed system is represented in Figure 1. First off, representative locations were identified along the perimeter of the industrial area, along with several

specific internal sites where hazardous emissions might potentially occur. Owing to the extension and complexity of the Mantova plant, covering some 300 acres and featuring complex metallic infrastructures, it was decided to subdivide the area involved in the piloting into 7 different subareas. Each subarea is covered by a subnetwork consisting of a Sink Node Unit (SNU) equipped with meteorological sensors, such as wind speed/direction and relative air humidity/temperature (eni1 to eni7 in Figure 1). In addition, the eni2 unit is further equipped with a rain gauge and a solar radiation sensor.

Each SNU is connected to one or more End Node Units (ENUs) equipped with VOC detectors (see Figure 2 for an example of a configuration), appropriately distributed across the plant's property. This modular approach allows the system to be expanded and/or reconfigured according to the specific monitoring requirements, while providing redundancy in case of failure of one or more SNUs. Since the potential sources of VOC emissions in the plant are located in well-identified areas, such as the chemical plant and the benzene tanks, the deployment strategy includes a number (6) of VOC sensors surrounding the chemical plant's infrastructure, thus resulting in a virtual fence capable of effectively evaluating VOC emissions on the basis of the concentration pattern around the plant itself.

The SNUs forward meteorological data, as well as VOC concentration data, to a remote server; as noted above, Internet connectivity is provided via TCP/IP over GPRS using a GSM mobile network. Wireless connectivity uses a UHF-ISM unlicensed band. Electrical power is provided by both primary sources (batteries) and secondary sources (photovoltaic cells), as mentioned above.

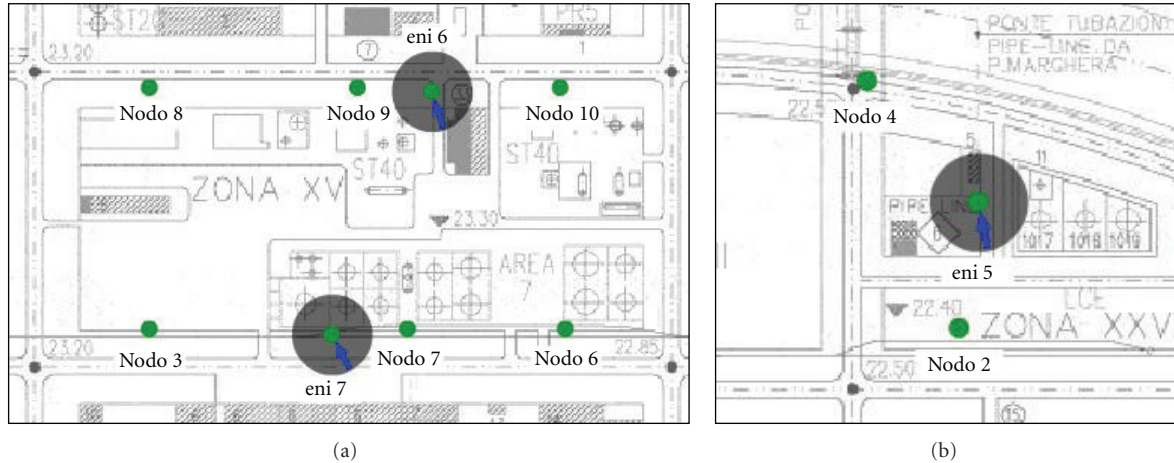


FIGURE 2: Closeups of SNU and ENU deployment around one of the chemical plants (a) and the pipeline (b). Maps are oriented according to plant's axes rather than cardinal directions.

VOC concentration and weather/climatic data are updated every minute. This intensive sampling interval allows the evolution of gas concentrations to be accurately assessed. Furthermore, when all of the weather-climatic measurements are collated, they provide a map of the area's relative air humidity/temperature (RHT) and wind speed/direction (WSD), which are crucial for providing accurate VOC-sensor read-out compensation [7]. The need for so many wind stations across the plant property is warranted by the turbulent wind distribution in the area, as can be observed by the different orientations of the blue arrows representing wind direction in Figure 1.

Three of the ENUs, eni1, eni2, and eni3, were deployed along the perimeter of the plant to locally monitor VOC concentration while correlating it with wind speed and direction; the other seven were placed around the chemical plant and in close proximity of the pipeline, which are possible sources of VOC emissions. Plans for extending the number of ENUs along the perimeter and to other chemical plants or potential sources of VOC emission are currently under consideration by PEM management.

In Figure 2 the layout of two of the subnetworks, one deployed around the chemical plant and one near the pipeline, are represented. The subnetwork around the chemical plant, Figure 2(a), consists of two SNUs, eni6 and eni7, equipped with weather sensors (air/wind), each connected with three ENUs spaced some fifty meters from each other. The subnetwork located in the pipeline area is shown in Figure 2(b); one of the two ENUs is located in close proximity of the end of the pipeline itself (*nodo 4*), while the other (*nodo 2*) is a bit further away. Sampling the VOC concentration at intervals of tens of meters allows the dispersion of VOC emissions to be evaluated; in addition, information about wind speed/direction allows the emission's source to be identified.

3. System Requirements

Given the hazardous and complex nature of the plant, developing a system that satisfied performance, reliability,

and nonintrusiveness/obtrusiveness, as well as scalability/reconfigurability requirements, was very challenging. Furthermore, as continuous power is crucial, efficient power saving strategies had to be implemented to prolong battery life. The major issues taken into account were the following.

Data Grid. In the presence of multiple, scattered sources (as in the case of VOCs in industrial sites), it is important to implement a grid monitoring network, in order to have simultaneously available data over the whole area of the plant. Furthermore, correlation with meteorological input allows workers to better interpret the data and more accurately pinpoint major emission sources.

Real-Time Acquisition. Continuous real-time data permits workers to immediately detect and, thus, effectively manage emergencies that may occur within the perimeter of the plant.

Data Rate. It is important to have a high sampling rate (i.e., a sampling interval of one minute or less) to determine the details during short-term situations, so as to formulate the most appropriate corrective actions.

Scalability and Reconfigurability. Network scalability and reconfigurability are key issues, particularly at complex industrial sites. In addition to deploying fixed stations (e.g., on the perimeter of the plant), it may be useful to be able to move the monitoring stations into specific areas during specific processing phases with potentially higher VOC emissions (e.g., startup, shutdown, revamping, etc.).

Data Rendering. Depending on the purpose of the monitoring (e.g., emergency management versus air quality monitoring, etc.), it is useful to make not only real-time VOC concentration data available, but also to provide statistical indices or cumulative patterns as well. This is cost effective for those situations, for example, in which specific information for a particular compound is not required.

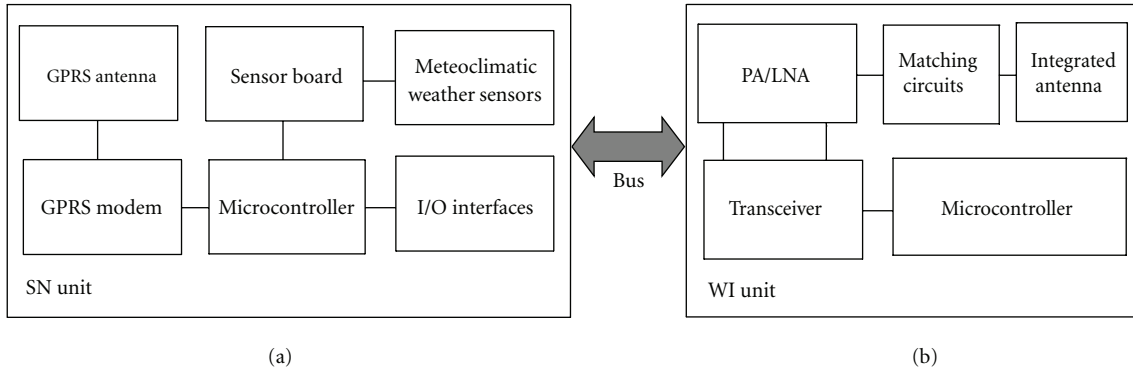


FIGURE 3: Block diagram of an SNU (a) and a WI unit (b).

Detection Threshold. If the purpose of monitoring is not only managing emergency situations, but also evaluating mean VOC concentrations for specific substances (in this case using the fixed monitoring stations), accordingly the choice should fall on detectors able to collect data at ppb concentration levels (as already mentioned, the air quality limit value for benzene in ambient air is currently about 1.5 ppb).

Communications. The use of wireless stations connected to a web-based graphic interface allows us to significantly reduce operating costs, as well as the costs for the infrastructure and the personnel involved.

4. The Communications Platform

The communications platform had to be able to support a scattered system of units collecting VOC emission data in real-time, while offering a high degree of flexibility and scalability, so as to allow for adding other monitoring stations as needed. Furthermore, it had to be reconfigurable, in terms of data acquisition strategies, while being more economically advantageous than traditional fixed monitoring stations.

The first requirement tackled in designing the platform was that of providing the SNU's with ubiquitous and reliable connectivity to Internet. At an early stage of the project, taking advantage of Ethernet, which was already available at some locations within the plant and which would use wireless access points to provide the SNU's with connectivity, was considered. This solution was dismissed, however, as it would have severely restricted the network's reconfigurability. The extent of the plant area, which required connectivity over several hundred square meters was another issue. Perhaps more important, however, was the presence of obstacles, such as trucks and metallic structures that could temporarily or permanently affect the communication channel.

A GSM mobile network solution was decided upon as the most suitable to fulfil the above requirements; it was implemented using a proprietary TCP/IP protocol with DHCP. Dynamic reconfigurability strategies were implemented to provide efficient and reliable communication with the GSM base station. All the main communication parameters, such

as IP address, IP port (server's and client's), APN, PIN code, and logic ID, can be remotely controlled. As for the wireless connectivity between the SNU's and ENU's, an unlicensed ISM UHF band (868 MHz) was selected. We shall now briefly explain the main components of the platform, the SNU's and the ENU's.

4.1. The SN and WI Units. In principle, a generic SNU consists of five components: a sensor unit, an analogue digital converter (ADC), a central processing unit (CPU), a power unit, and a communication (Wireless Interface) unit. The communication unit's task is to receive a command or a query and then transmit that data from the CPU to the outside world. The CPU is the most complex unit; it interprets the command or query to the ADC, monitors and controls power if necessary, processes received data, and manages the EN wake-up.

The block diagram of the SNU is represented in Figure 3(a). It consists of a GPRS antenna and a GPRS/EDGE quadband modem, a sensor board, an I/O interface unit, and an ARM-9 microcontroller operating at 96 MHz.

The system is based on an embedded architecture with a high degree of integration among the different subsystems. The unit is equipped with various interfaces, including LAN/Ethernet (IEEE 802.1) with TCP/IP protocols, USB ports, and RS485/RS422 standard interfaces. The sensor board is equipped with 8 analogue inputs and 2 digital inputs. The SNU is also equipped with a Wireless Interface (WI), shown in Figure 3(b), which provides connectivity with the ENU's.

The WI, Figure 3(b), provides short-range connectivity. The WI operates on low-power, ISM UHF unlicensed band (868 MHz) with FSK modulation; it features proprietary hardware and communication protocols. Distinctive features of the unit are the integrated antenna, which is enclosed in the box for improved ruggedness, as well as a PA + LNA for a boosted link budget. The PA delivers 17 dB m to the antenna, while the receiver's noise figure was reduced to 3.5 dB, compared with the intrinsic 15 dB NF of the integrated transceiver. As a matter of fact, a connectivity range in line-of-sight in excess of 500 meters was obtained, with a reliable communication with a low BER, even in hostile EM environments.

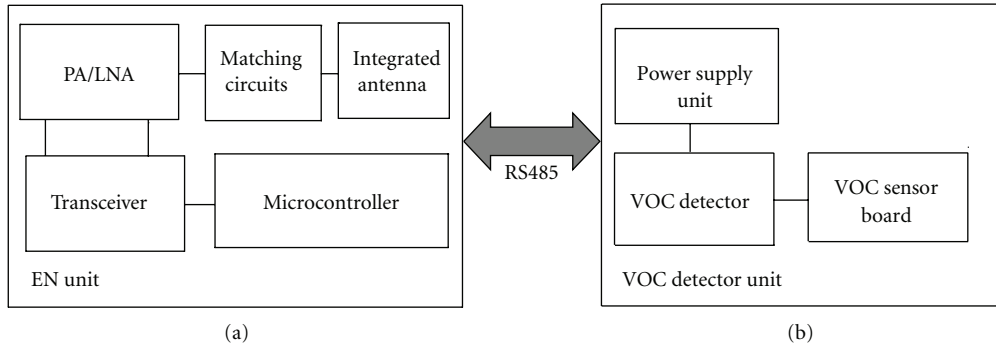


FIGURE 4: Block diagram of the End Node Unit (left) and the VOC detector unit (right).

The energy required for the unit's operation is provided by an 80 Ah primary source and by a photovoltaic panel equipped with a smart voltage regulator. Owing to its careful low-power design, the unit could be powered with a small (20 W) photovoltaic panel while maintaining continuous, unattended operation.

4.2. The EN Unit. The block diagram of the EN is shown in Figure 4; it consists of a WI, similar to that previously described, and includes a VOC sensor board and a VOC detector. The acquisition/communication subsystem of the ENU is based on an ARM Cortex-M3 32-bit microcontroller, operating at 72 MHz, which provides the necessary computational capability on the limited power budget available.

To reduce the power requirement of the overall ENU subsystem, two different power supplies have been implemented, one for the microcontroller and one for the peripheral units; the microcontroller is able to connect/disconnect the peripheral units, thus preserving the local energy resources. The VOC detector subsystem in particular is powered by a dedicated switching voltage regulator; this provides a very stable and spike-free energy source, as required for proper operation of the VOC detector itself.

The communication between the ENU and the VOC detector board is based on an RS485 serial interface, providing high-level immunity to interference as well as bidirectional communication capability, which is needed for remote configuration/reconfiguration of the unit.

5. WSN Issues

5.1. Network Structure and Routing Schemes. Among the different alternatives, a hierarchical-based routing scheme was selected based on the particular nature of the installation: the extended area of the plant, the few critical areas of potential sources of emissions requiring a dense deployment, and the highly uneven distribution of nodes over the area. A hierarchical-based routing scheme fits the projected deployment layout well. As said before, the installation was partitioned into subnetworks to be deployed around the critical sites, with one SNU for each individual subnetwork. In principle, wireless connectivity between the SNUs could have been implemented, using one specific SNU as a gateway

to the Internet. This option, however, conflicted with at least two of the major requirements. The first is the need for redundancy in case of failure of the gateway unit; in this scenario, in fact, Internet connectivity would be lost, with consequent loss of the real-time updating capability, which is considered a mandatory requirement of the system. The second need which would not have been met is that of providing full connectivity among the individual SNU under conditions where line-of-sight propagation was not guaranteed, due to the presence of such temporary obstacles as trucks or maintenance infrastructures. A multiple GPRS gateway approach overcomes those limitations; even in the case of failure of one or more gateway units, Internet connectivity would be provided by the others still in operation, while the issue of the obstacles is circumvented. As for the wireless connectivity, a star configuration was preferred to a mesh configuration, given the limited number of nodes and the need to keep latency at a minimum.

5.2. Protocols and WSN Services. Two levels of communication protocols, in a mesh network topology, were implemented. The upper level handles communications between the SNs and the server; it uses a custom binary protocol on top of a TCP layer. This level was designed and calibrated for real-time bidirectional data exchange, where periodic signaling messages are sent from both sides. Since our sensor network necessitates a stable link, quick reconnection procedures, for whenever broken links should occur, were especially important. To ensure minimal data loss, the SNs have non-volatile data storage, as well as automatic data packet retransmission (with timestamps) after temporary downlink events. Furthermore, this design is well suited for low-power embedded platforms like ours, where limited memory and power resources are available. In fact, our protocol stack currently requires about 24 KB of flash memory (firmware) and 8 KB RAM.

The lower level, in contrast to the upper one, concerns the local data exchange between the network nodes. Here a cluster tree topology was employed; each node, which both transmits and receives data packets, is able to forward packets from the surrounding nodes when needed. In this specific application, the topology and routing schemes are based on an ID assigned to each EN unit, where the ID can be

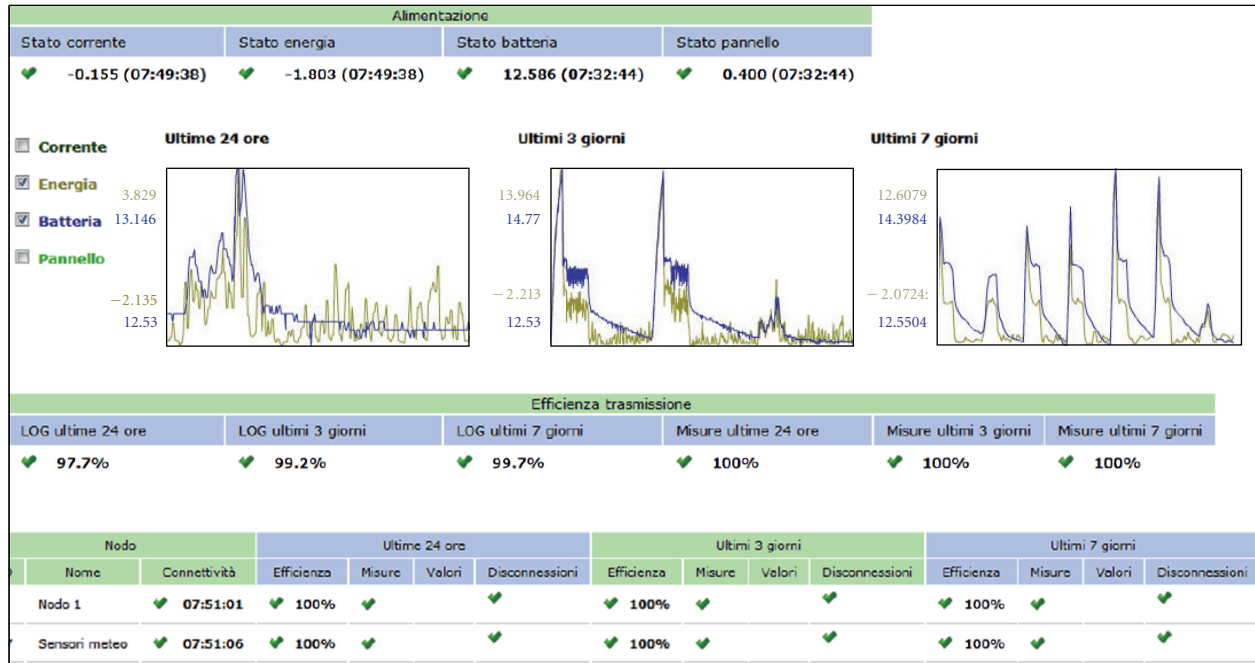


FIGURE 5: Block diagram of the ENU (left) and the VOC detector unit (right) connectivity and power supply.

easily adjusted using selectors on the hardware board. This choice allows for easy support and maintenance, even when nonspecialized operators have to install, reinstall or service one or more units.

5.3. Reliability and Energy Balance. The reliability of the system and capability for stand-alone operation are summarised in Figure 5, where the main connectivity and power-supply parameters are displayed for one of the SNU.

The energy balance and battery voltage are charted in the upper panel, from left to right, for one, three and seven days, from October 13th to 20th; hence, the net energy balance was obtained for the middle of October. GPRS connectivity performance, displayed in the middle panel, shows a reliability in excess of 99%. Wireless connectivity and data communication performance are displayed in the lower panel; no disconnection or data loss is observed in that period.

6. Energy Budget Issues

Energy budget plays a key role in the maintainability of the WSN [8]. In our case this is made even more critical by the necessity for stand-alone operation, as well as due to periodic maintenance intervals exceeding four months. Since electrical energy from the plant could not be used, secondary sources had to be locally available; photovoltaic panels (PVP) fit the bill. The SNU are almost all equipped with PVPs, as they have to support a number of functions, including connectivity and data collection from sensors. The ENUs, when equipped with low-energy demanding sensors, have 3 to 5 years of battery life using primary sources [9]. However, in this installation the ENUs have to support the

power-hungry VOC sensors. For this reason, the ENUs are also equipped with PVPs.

6.1. ENU Energy Budget. The EN nodes have been fully deployed since July 2011; since that time we have noticed that the VOC sensor energy budget is predominant compared to that of the computational/communication unit. This is a critical issue for the ENUs, as the PIDs used for reading the VOC concentration need to be continuously on to operate efficiently. This corresponds to a current draw of some 30 mA, corresponding to 720 mA h a day, more than twice the amount the communication/computational units, with their power consumption of some 360 mW a day, require. The ENU's primary source capacity is 60 Ah, which provides more than 2 full months of continuous operation.

To rely on autonomous energy resources, while providing continuous operation, a secondary energy source was integrated into the ENU in order to supply the 360 mW average required power. A 5 W photovoltaic panel can fulfil the task only under ideal sunlight conditions, that is, in summer, but hardly at all in winter. The photovoltaic power supply unit includes a charge regulator which was specifically designed to provide maximum energy transfer efficiency from the panel to the battery under any operative condition. Furthermore, the secondary energy source plays a key role in ensuring the stand-alone and unattended operation of the communication platform.

In Figure 6 the battery voltage plots are shown for the ENUs connected to SN 5 and 6. As it can be observed, the ENUs exhibit quite satisfactory charge conditions. ENU 4 (eni5 nodo 4) exhibits a slightly lower voltage level, probably due to a deployment in a partially shadowed area. The battery voltage remains above a 12.3 V value, with a slight decreasing

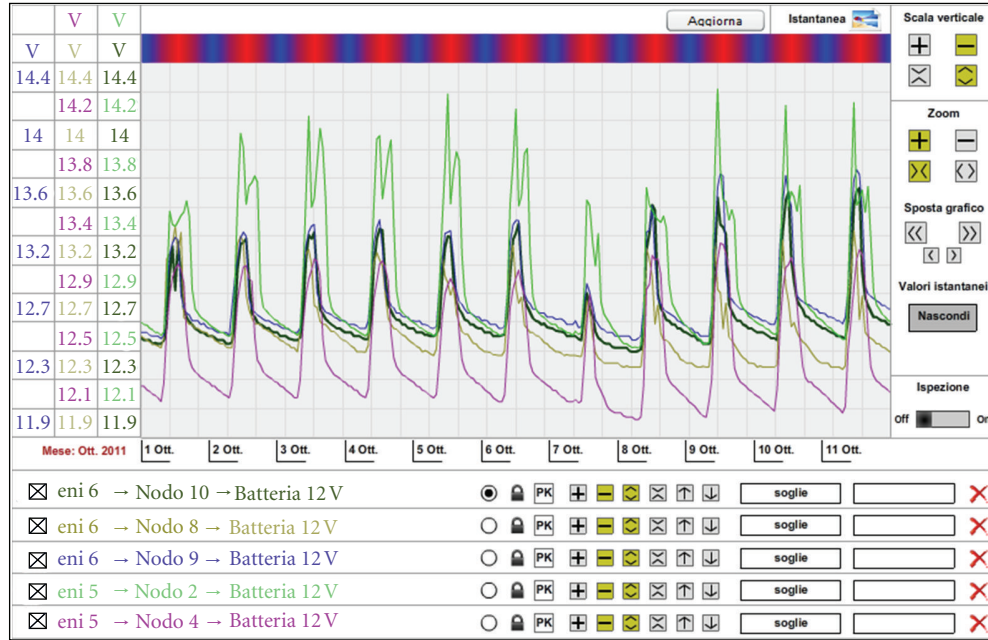


FIGURE 6: Battery voltage of the ENUs of the eni6 and eni5 subnetworks from October 1st to October 11th.

trend, possibly due to the lower solar energy because of the onset of autumn.

6.2. SNU Energy Budget. The SNUs were deployed at the PEM plant in the middle of April 2011; they have much higher energy requirements than the ENUs as they have to supply energy both for wireless connectivity and sensor operation.

The average current draw is around 90 mA, corresponding to a power consumption of about 1 W. SNUs have superior primary and secondary resource capabilities, with a 2-month battery life relying only on the primary source.

Figure 7 shows the battery voltage for the eni2 to eni7 SNUs; the eni1 plot is missing as the graph can only represent 6 graphs in each diagram. As can be observed, all the units demonstrate a minimum voltage exceeding 12.3 V, which denotes a satisfactory charge condition. In the above period there is also a slight decrease in the minimum battery voltage value, showing an energy imbalance between the primary and secondary sources, mostly due to sunlight reduction.

Detailed information about the charge status and trending are also available; in Figure 8 the current drawn by or supplied to the battery is compared with the charge status of the primary source. In this case, the energy balance keeps the battery voltage at a steady satisfactory level. Extensive data logs and reports are available to help the maintenance team in evaluating any critical event or service required to keep the system in full operation.

7. The VOC Detector

The VOC detector is a key element for the monitoring system's functionality. For this application two criteria were

TABLE 1: System requirements.

VOC data sampling interval (minutes)	≤15
Power consumption (mW)	<200
Stabilisation time from power-on: T90 (seconds)	<60
Warm-up time (seconds)	<60
Interval between services (days)	>120
Lifetime (years)	>5
Specificity to benzene	Typically broad band

considered mandatory. The first is that the VOC detector should be operated in diffusion mode, thereby avoiding pumps or microfluidic devices which would increase the energy requirements and make the maintainability issues more critical. The second criteria was that they system should be able to operate in the very low part per billion (ppb) range, with a Minimum Detectable Level (MDL) of some 2.5 ppb with a $\pm 5\%$ accuracy in the 2.5 to 1000 ppb range, which represents the range of expected VOC concentration.

Other requirements for the VOC detectors are listed in Table 1.

An extensive analysis of the state-of-the-art devices was performed to identify the most suitable technology among the many alternatives offered by the market. Among the different candidates, which included Photo Ionisation Detectors (PID), Amperometric Sensors, Quartz Crystal Microbalance (QMC) sensors, Fully Asymmetric Ion Mobility Spectrography (FAIMS) based on MEMS, Electrochemical Sensors, and Metal Oxide Semiconductor Sensors (MOSS), it turned out that the PID technology fitted our criteria quite well, and thus it was selected as the basis for our system. The specific

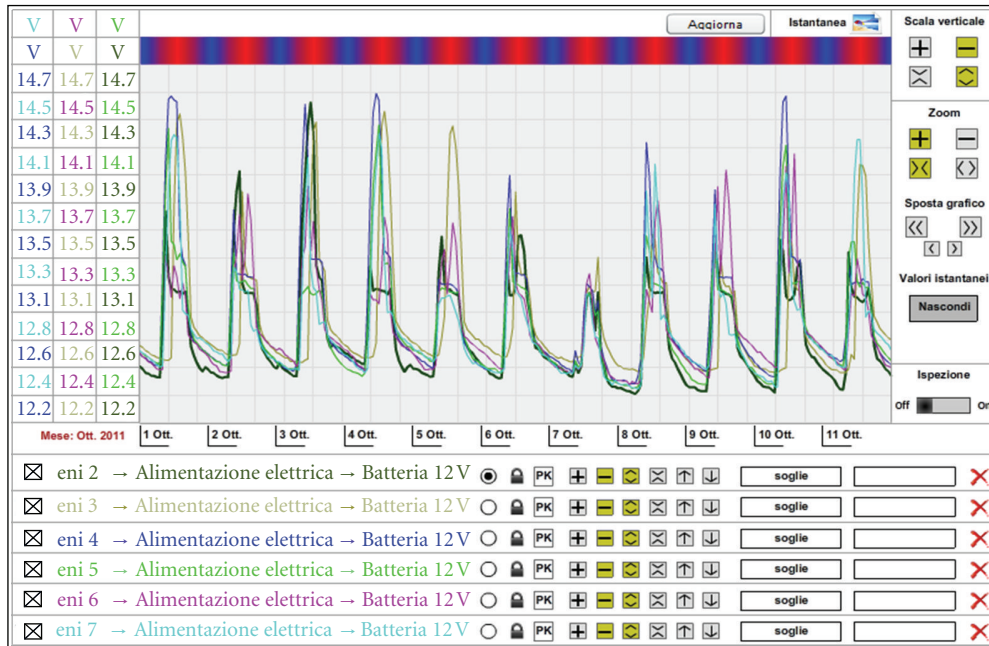


FIGURE 7: Battery voltage of SNUSNUs 2 to 7 in the period October 1st–October 11th.



FIGURE 8: Current and charge status of SNU 1 from October 1st to October 11th.

device chosen was the Alphasense PID AH, which has an MDL of 5 ppb (for isobutylene) and 2.5 ppb for benzene, whose response factor is 0.5.

Both theoretical and experimental investigations of PID operation [10, 11] were carried out to assess the PID AH's performance. Two major issues were identified which could potentially affect efficient use of the PID in our system. The first was that in the low ppb range the calibration curve of the PID shows a marked nonlinearity; this would require an individualized, meticulous multipoint calibration involving

higher costs and complexity. The second issue was that, when operated in diffusion mode at low ppb and after a certain time in power-off, the detector required a stabilisation time of several minutes, hence it would not be able to operate at our required one-minute intervals.

Since both of the above-mentioned limitations are intrinsically related to the PID's physical behaviour, this was carefully investigated and a behavioural model of the PID was developed to explain these phenomena. Moreover, a mathematical expression of the PID calibration curve was

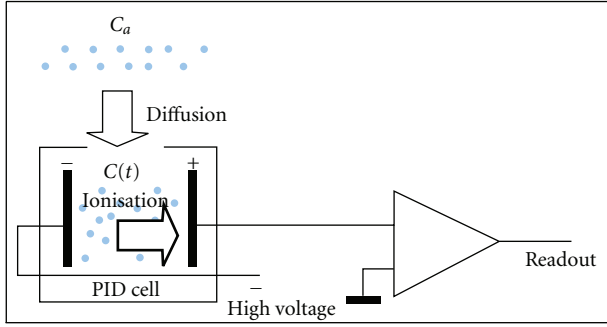


FIGURE 9: Basic operation of the PhotoIonisation Detector (PID).

derived. Although the theory has not been published yet [12], a brief explanation will be given here to justify the assumptions made in the design of the VOC detector unit.

With reference to Figure 9, the PID consists of a cell where an Ultraviolet (UV) lamp and two electrodes have been placed; a high voltage is established between the electrodes, generating an electric field while a hole puts the cell in direct contact with the atmosphere.

The basic operation of the PID can be described as follows. Let us assume the PID is immersed in an atmosphere containing molecules of a gas with an Ionization Potential (IP) that is lower than the energy of the photons emitted by the UV lamp; in that case an ionisation process takes place. Ions and electrons produced by the process then give rise to a drift current and are collected by the two electrodes; since each current corresponds to a specific gas concentration, the device is able to give a readout of the gas concentration within the cell. The ionisation process, by lowering the gas concentration in the cell, determines a diffusive process to take place, causing molecules to move from outside to inside the cell. It has been shown in the above-mentioned theory that at low ppb concentration levels, and when the PID is operated in diffusion mode, the rate at which the molecules diffuse is lower than that at which they are ionised. Consequently, when a stable readout is achieved, the concentration inside the cell, C_i , is somewhat lower than the concentration outside, C_a ; in that condition, the readout voltage proportional to the drift current generated by the ionisation process is given by:

$$V_r = S_v C_i, \quad (1)$$

where S_v represents the PID sensitivity expressed in mV/ppm, and V_r is the read-out voltage.

The PID calibration curve defines the relationship between the measured voltage and environmental gas concentration. It is given by:

$$V(C_a) = S_v C_a. \quad (2)$$

Inspection of Formula (2) shows that, at low ppb concentrations where $C_i \neq C_a$, a correction factor is needed to appropriately map the read-out voltages onto the environmental concentration.

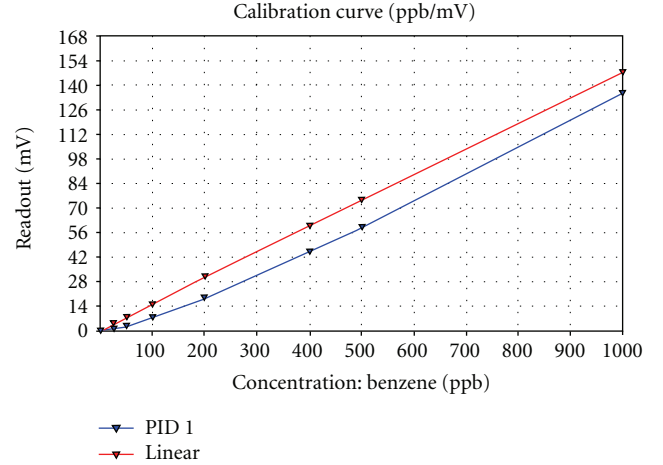


FIGURE 10: Experimental (blue) and linearised (red) calibration curve of the Alphasense PID AH.

7.1. PID Calibration. It is shown in [13] that at ppm concentrations the PID calibration curve is practically linear. PID calibration in the ppm concentration range is usually performed by measuring the slope of the calibration curve, S_v , at ppm concentrations; the measured read-out values are then easily mapped onto the corresponding environmental concentration values, according to (2).

This straightforward procedure cannot be used in the ppb concentration range, owing to the nonlinear behaviour of the relationship between read-out voltages and environmental concentration, thus requiring an individualized, careful and multipoint calibration to be implemented, with additional costs and complexity. To overcome this limitation, a linearisation procedure for the ppb concentration range was developed, based on a behavioural model of the PID.

Accordingly, the voltage readouts measured by the detector, $V_r(C_a)$, are first multiplied by a nonlinearity compensation factor, $\gamma(C_a)$, a function of the environmental concentration C_a , according to the following expression:

$$V(C_a) = \gamma(C_a) V_r(C_a). \quad (3)$$

As a result, a linear calibration curve is obtained for the ppb concentration range, allowing the environmental concentration values to be attained by the measured read-out values, according to expression (3). The result of this process is shown in Figure 10, where the experimental function $V_r(C_a)$ is represented by the blue line, and the results of the linearisation process are represented by the red line.

7.2. PID Stabilisation Time. The second problem arising from PID operation is represented by the stabilisation time required to achieve a stable read-out time in diffusion mode at low concentrations (tens or hundreds of ppb), which represents the area of operation of the VOC detectors for our application. This effect is clearly shown in the experiment in Figure 11.

In the experiment, C_a was around 50 ppb, which represents the average concentration where the PID is supposed

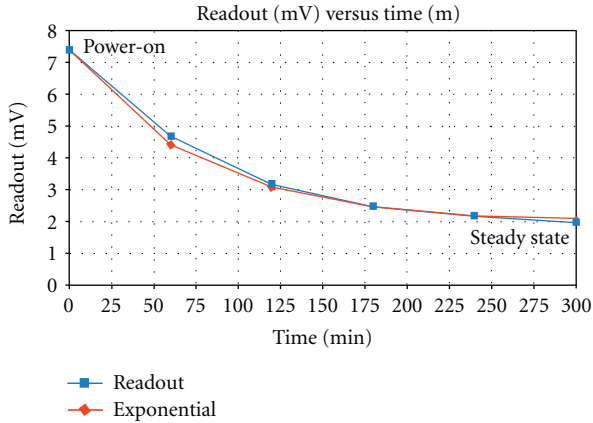


FIGURE 11: PID stabilisation time after power-on.

to be set up. At time $t = 0$, the PID was powered-on and the readout was sampled at a 1 minute interval. The PID readout (blue line), is compared with an 80-second time-constant exponential curve (red line), showing a very good agreement. The reason for the relatively high stabilisation time at low ppbs is related to the same phenomenon that gives rise to a nonlinear calibration curve, that is, that a stable readout is obtained when the concentration inside the cell is lower than the environmental concentration. This effect is clearly observed in Figure 10; at power-on the read-out voltage of the ionisation process is proportional to C_a , which is higher than C_i . With the progression of the ionisation process, C_i decreases and eventually reaches a stable value.

The PID's stabilisation time highly impacts the device's operation. According to the specifications of Table 1, a minimum VOC data sampling interval of at least fifteen minutes is required. Furthermore, a duty-cycled operation is desirable, in principle, to prolong the battery life. Operating the detector on a fifteen minute duty-cycle basis, and taking into account the stabilisation time, the benefit in terms of maintenance effort is marginal and has to be compared with the advantage of achieving a more time-intensive monitoring of VOC concentration, as provided by continuous power-on operation. Accordingly, it was decided to operate the VOC detectors continuously at one-minute data sampling; this decision proved to be very effective, as some emission events at the plant show very rapid variation, which could result in a difficult interpretation at ten-minute sampling rates.

Continuous power-on operation requires a 35 mA h charge, which corresponds to about 2 months of full operation with a 60 A h primary energy source. On the other hand, the UV lamp's expected life is more than 6000 hours of continuous operation, that is, four months at least. Consequently, a four-month routine maintenance is planned for the system, so that UV lamp replacement, PID refitting, and battery replacement can be appropriately scheduled.

8. Experimental Results

Data gathered from the field are forwarded to a central database for data storage and data rendering. A rich and

proactive user interface was implemented in order to provide detailed graphical data analysis and presentation of the relevant parameters, both in graphical and bidimensional format. Data from the individual sensors deployed on the field, either microclimatic or VOC, can be directly accessed and presented in various formats.

Information at a glance is provided by the map in Figure 12(a). As explained in Figure 1, the SNU's of the individual subnetworks are represented as grey circles with a blue arrow indicating the wind direction. By positioning the mouse pointer over an SNU icon, all of its microclimatic and VOC parameter values are displayed. As shown in Figure 2, a closeup of subnetworks can be accessed, for detailed information of VOC concentration readout at each ENU.

A summary of the sensor status for each deployed unit can be obtained by opening the summary panel, Figure 12(b). The summary panel reports current air temperature/humidity values, along with min/max values of the day (lower left in Figure 12(b)), wind speed and direction (upper left in Figure 12(b)), and VOC concentration (bar chart on right-hand side of Figure 12(b)) over the last six hours.

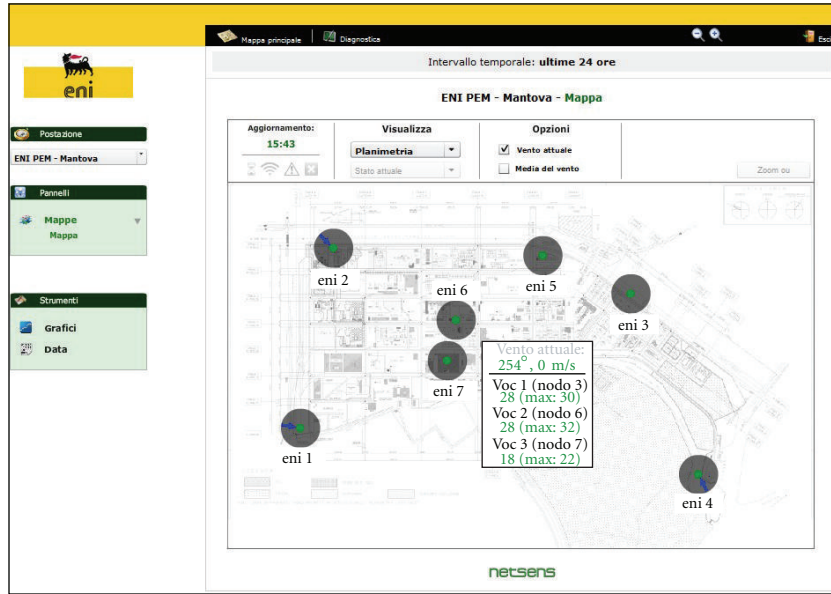
In Figure 13 a comprehensive 2D representation of the VOC, Figure 13(a), and climatic, Figure 13(b), parameter distribution over the plant is shown.

The representations were obtained using an interpolation algorithm in pseudocolour. Blue denotes a lower concentration/temperature, while red indicates a higher one. It should be emphasized that the choice of red was merely a chromatic one; it has absolutely no reference to any risky or critical condition.

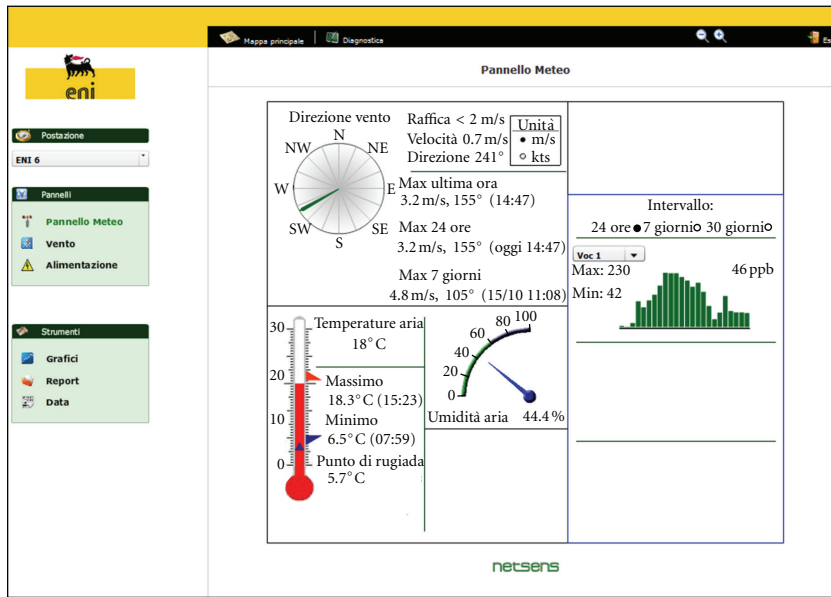
A graphic representation of data gathered by each sensor on the field can be obtained by opening the graphic panel window, see Figure 14. This panel allows anyone to display the stored data in any time interval in graphic format; up to six different and arbitrarily selected sensors can be represented in the same graphic window for purpose of analysis and comparison. In Figure 14, for example, the six traces represent the VOC concentration values detected by the six PIDs deployed around the chemical plant. The optimum uniformity among the background concentration levels should be noted, as it demonstrates the effectiveness of the calibration procedure.

The background values range from 50 to 150 ppb. Thanks to the intensive 1-minute sample interval, the evolution of the concentration, along with other relevant weather parameters, can be accurately displayed. It should be noted that the spikes that can be observed in the traces have an average duration of 2-3 minutes.

When VOC sources need to be identified, the correlation between wind/speed direction and VOC concentration is vital. In Figure 15 two different representations of VOC concentrations combined with the wind direction data are shown for two detectors located at the plant perimeter, namely, ENUs 1 and 2. The plot, in polar coordinates, represents the wind directions referenced to the North and the VOC concentration in ppb. The diagram shows the average VOC concentration in all directions, as detected by



(a)



(b)

FIGURE 12: Examples of data rendering: installation map (a) and summary panel (b).

the PID during a full day. The plot gives an overview of the predominant orientation of the VOC flux during the day.

In Figure 15(a) the diagram of ENU 1, located in the southwest corner of the plant, is shown. The area outside the plant is to the west, while the area inside is to the east of ENU 1. In Figure 15(a) the VOC concentration is higher in quadrants I and IV, showing that the net VOC flow is entering the plant area. This may be related to the emissions generated by the traffic on the motorway running along the west side of the plant, or possible emissions from other industrial sites.

Across the motorway there are also a petroleum refinery (WSW) and its storage area (WNW). The same diagram for

ENU 2, which is instead located at the northwest corner of the plant, is shown in Figure 15(b). Here the opposite situation is found, as the highest concentration values are in the II quadrant. It should be noted, however, that the data for ENU 2 was recorded on a Sunday when the traffic is assumed to be less intense.

9. Conclusions

An end-to-end distributed monitoring system of integrated VOC detectors, capable of performing real-time analysis of gas concentration in hazardous sites at an unprecedented

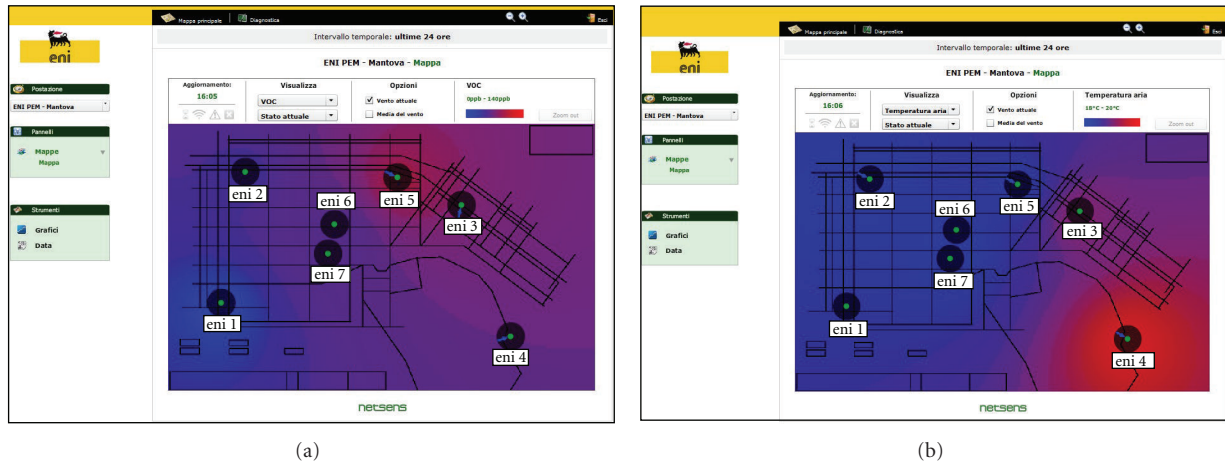


FIGURE 13: Examples of data rendering: VOC concentration (a) and temperature distribution (b) across plant site.

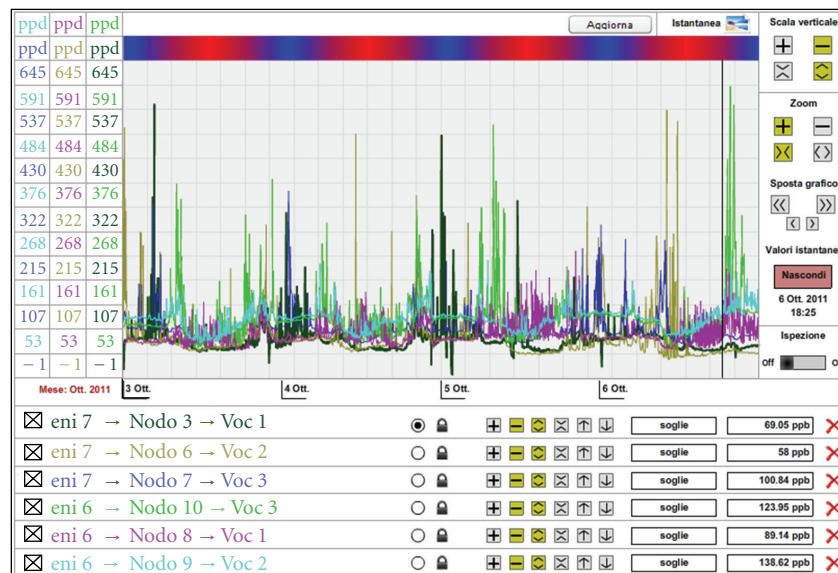


FIGURE 14: Example of data rendering: Graph of VOC concentration in the six detectors deployed around the chemical plant.

time/space scale, has been implemented and successfully tested in an industrial site. The aim was to provide the industrial site with a flexible and cost-effective monitoring tool in order to achieve a better management of emergency situations, to identify emission sources in real time, and to collect continuous VOC concentration data using easily redeployable and rationally distributed monitoring stations.

The piloting of the system allowed us to pinpoint key traits. Collecting data at 1-minute time intervals meets several needs: identifying short-term critical events, quantifying the emission impacts as a function of weather conditions as well as of operational process, in addition to identifying potentially VOC sources in the plant area. Moreover, the choice of a WSN communication platform gave excellent results, above all in allowing for redeploying and rescaling the network's configuration according to specific needs

as they arise, while, at the same time, greatly reducing installation costs. Furthermore, real-time data through a web-based interface allowed both adequate levels of control and quick data interpretation in order to manage specific situations. In terms of the actual detectors, among the various alternatives available on the market, PID technology proved to meet all the major requirements, as PIDs are effective in terms of energy consumption, measuring range, cost, and maintenance once installed in the field. Finally, fitting weather sensors at the nodes of the main network stations allowed for a clearer understanding of on-field phenomena and their evolution, thus providing accurate identification of potential emission sources.

Future activity will include a number of further developments, primarily the development of a standard application to allow the deployment of WSN in other network industries

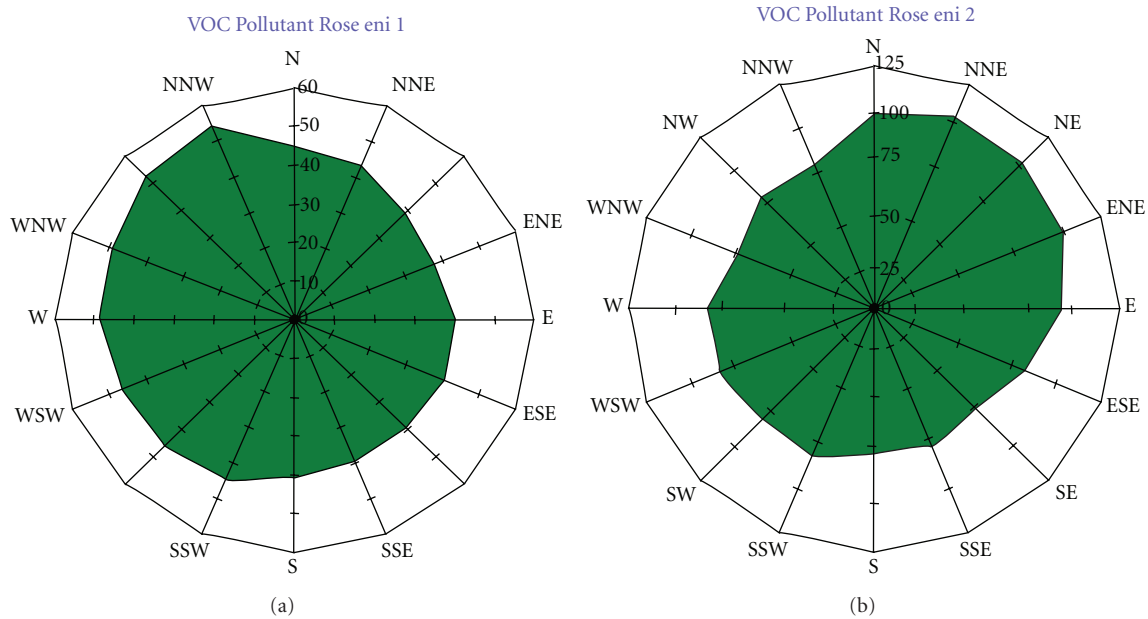


FIGURE 15: Example of data rendering: correlation between wind and VOC concentration for ENU 1 (a) and 2 (b).

(e.g., refineries) in addition to an assessment of potential applications for WSN infrastructure monitoring of other environmental indicators.

Acknowledgments

This work was supported by eni S.p.A. under contract no. 3500007596. The authors wish to thank W. O. Ho and A. Burnley, at Alphasense Ltd., for their many helpful comments and clarifications concerning PID operation, as well as E. Benvenuti, at Netsens s.r.l., for his valuable technical support. Assistance and support from the management and technical staff of Polimeri Europa Mantova is gratefully acknowledged. The valuable support by Mrs J. A. Thonn for revising the English is also acknowledged.

References

- [1] G. Manes, R. Fusco, L. Gelpi, A. Manes, D. Di Palma, and G. Collodi, *Real-Time Monitoring of Volatile Organic Compounds in Hazardous Sites*, chapter 14, Intech Book, Environmental Monitoring, 2011.
- [2] W. Tsujita, H. Ishida, and T. Moriizumi, "Dynamic gas sensor network for air pollution monitoring and its auto-calibration," in *Proceedings of the IEEE Sensors*, vol. 1, pp. 56–59, October 2004.
- [3] F. Tsoy, E. Forzani, A. Rai et al., "A wearable and wireless sensor system for real-time monitoring of toxic environmental volatile organic compounds in," *IEEE Sensors Journal*, vol. 9, no. 12, pp. 1734–1740, 2009.
- [4] S. Choi, N. Kim, H. Cha, and R. Ha, "Micro sensor node for air pollutant monitoring: hardware and software issues," *Sensors*, vol. 9, no. 10, pp. 7970–7987, 2009.
- [5] R. Szewczyk, A. Mainwaring, J. Polastre, J. Anderson, and D. Culler, "An analysis of a large scale habitat monitoring application," in *Proceedings of the 2nd International Conference on Embedded Networked Sensor Systems*, pp. 214–226, November 2004.
- [6] R. Adler, P. Buonadonna, J. Chabra et al., *Design and Deployment of Industrial Sensor Networks: Experiences from the North Sea and a Semiconductor Plant in ACM SenSys*, San Diego, Calif, USA, 2005.
- [7] MiniPID User Manual V1.8, IonScience Ltd, 2000.
- [8] J. Jeong, D. E. Culler, and J. H. Oh, "Empirical analysis of transmission power control algorithms for wireless sensor networks," in *Proceedings of the 4th International Conference on Networked Sensing Systems (INSS '07)*, pp. 27–34, IEEE Press, June 2007.
- [9] G. Manes, R. Fantacci, F. Chiti et al., "Energy efficient MAC protocols for wireless sensor networks endowed with directive antennas: a cross-layer solution," in *Proceedings of the IEEE Radio and Wireless Conference*, pp. 239–242, Orlando, Fla, USA, January 2009.
- [10] J. G. W. Price, D. C. Fenimore, P. G. Simmonds, and A. Zlatkis, "Design and operation of a photoionization detector for gas chromatography," *Analytical Chemistry*, vol. 40, no. 3, pp. 541–547, 1968.
- [11] D. C. Locke and C. E. Meloan, "Study of the photoionization detector for gas chromatography," *Analytical Chemistry*, vol. 37, no. 3, pp. 389–395, 1965.
- [12] G. F. Manes, unpublished results.
- [13] Alphasense Ltd., Technical specifications; Doc. Ref. PID-AH/MAR11.



Hindawi

Submit your manuscripts at
<http://www.hindawi.com>

